

THE EFFECT OF VERY HIGH HYDRAULIC PRESSURE ON THE PERMEABILITY AND SALT REJECTION OF REVERSE OSMOSIS MEMBRANES

Authors: *Ronan Killian McGovern, Dillon McConnon and John H. Lienhard V*

Presenter: *Ronan Killian McGovern, PhD*
Post-doctoral Associate – Massachusetts Institute of Technology – USA
mcgov@alum.mit.edu

Abstract

We employ a stirred-cell reverse osmosis setup to demonstrate that a seawater reverse osmosis membrane can maintain excellent salt rejection at pressures as high as 172 bar. However, we also demonstrate a very significant drop in membrane permeability at high pressures – likely due to membrane compaction. At 172 bar, permeability is more than 50% lower than at a pressure of 34.5 bar. In addition, our results illustrate how flux fluctuates significantly in time when the pressure is removed and then reapplied, even for very short periods, in high pressure reverse osmosis processes – an effect that requires careful consideration from the perspective of process control and operation. From the perspective of membrane performance, RO is feasible at high pressures but distinct challenges are presented by reduced permeability and increased variability in flux.

I. INTRODUCTION

We demonstrate, using a high pressure stirred cell, that seawater reverse osmosis (RO) membranes can reject salt effectively, even when operating at pressures of up to 172 bar. Although water permeability is reduced relative to performance at conventional seawater test pressures of 55 bar, salt rejection is improved. These results are significant as they demonstrate that, at least from the perspective of membrane performance, reverse osmosis systems can treat waters with osmotic pressures that go far beyond seawater salinities.

One application of relevance to high pressure reverse osmosis systems is the purification of waters in the oil and gas industry, where certain highly saline waste water streams require purification [1]. The use of reverse osmosis, which is by far the most energy efficient desalination technology for seawater desalination [2], is particularly interesting given the poor energy efficiency of the thermal technologies currently employed for the desalination of highly saline waters [3]. If feasible, high salinity reverse osmosis systems could potentially achieve significant reductions in energy consumption relative to mechanical vapour compression systems [3].

Of relevance to the feasibility of RO at high pressures is the question of whether RO membranes can perform satisfactorily, in terms of water permeability and salt rejection, at high pressures. Until now, answers to this question have been largely theoretical. Studies on the effect of hydraulic pressure on thin film composite polyamide membranes have, to our knowledge, been limited to experiments spanning pressures up to 50 bar on nano-filtration (NF) membranes [4,5] and preliminary experiments reaching 69 bar on reverse osmosis membranes [6].



In brief, our expectations for the performance of reverse osmosis at high pressures are perhaps well summarized by the following three observations of studies conducted to date in literature:

1. Reverse osmosis membranes comprise three layers – a porous fabric, a polysulfone support layer and a salt-rejecting polyamide layer, known as the active layer. The polyamide active layer is the thinnest of all layers (~200 nm) and sits upon the porous polysulfone layer. At high pressures, there is therefore concern that the active layer might tear and compromise the salt rejecting ability of the membrane. Synthesis and analysis of thin film composite membranes, achieved via pendant drop mechanical analysis, indicates that the rupture stress of the active layer is on the order of 400 bar [7]. While it would be incorrect to directly compare this rupture stress to the hydraulic pressure applied, it is nonetheless comforting that the rupture stress is on the order of 400 bar – perhaps suggesting the membrane is robust at very high pressures.
2. Analysis of the permeability and salt rejection of nanofiltration membranes indicates that as hydraulic pressure increases, permeability to water decreases but salt rejection increases [4,5]. Furthermore, it appears that there exists a value of applied hydraulic pressure at which flux reaches a limiting value [4]. The active layer composition in nanofiltration membranes is certainly different than for reverse osmosis – indeed the active layer in NF appears to be more aromatic, less rough, less hydrophobic, and less homogeneous than the active layer in an RO membrane [8,9,10]. Nonetheless, it is interesting to ask whether permeability and salt rejection might follow the same trends for RO at high pressure as seen for NF and whether a limiting value of flux might exist.
3. Finally, in assessing the pressure dependence of flux for NF membranes, a viscoelastic model (spring and damper in parallel) was shown to fit the evolution of permeability of water with time during the application of a fixed hydraulic pressure [5]. It is therefore interesting to ask whether such a model might adequately describe the evolution of permeability with time for RO and, furthermore, whether such a model remains accurate during the repeated application and removal of pressure.

II. METHODS

Experimental

De-ionised water with a conductivity of less than 5 $\mu\text{S}/\text{cm}$ was used in all experiments (McMaster Carr, New Jersey, USA). The membranes used in all experiments were SWC membranes from Hydranautics (California, USA). The membranes were obtained as hydrated flat sheets in a sodium bisulfite solution. These membranes were cut from seawater RO elements that had previously been operated at standard seawater test conditions for a period of 30 minutes. Each sample was used for one experiment only.

A dead-end, stirred cell (HP4750X; Sterlitech, Washington, USA) was used for permeability and rejection studies. The cell is made of stainless steel and withstands pressures of up to 172 bar. The cell accommodates a stirring bar that is suspended above the membrane without making contact. The membrane was secured against an EPDM O-ring and the torque applied to the bolts was 20ft-lbs. Pressure was applied using a nitrogen cylinder connected to the cell, a pressure regulator (Y11-N198J; Airgas, Radnor, PA, U.S.A.) and a pressure gauge (345 bar rating; Ashcroft, Stratford, CT, U.S.A.). During tests, pressure fluctuated by no more than ± 7 bar. Water flux determined by measuring the mass of permeate versus time using a precision scales (ML203E; Mettler Toledo, Billerica, MA, U.S.A.). Flux was based upon a 750 second time average. Permeability was computed by dividing the water flux by the applied



hydraulic pressure, adjusting for the osmotic pressure at the surface of the RO membrane where necessary (Eq. 1).

$$\text{Eq. 1: } J_w = A_m \left[P - \pi \exp\left(\frac{J_w}{k}\right) \right]$$

J_w is the water flux, A_m is the permeability of the membrane to water, π is the osmotic pressure of the solution and k is the mass transfer coefficient resulting from stirring. For the purpose of calculations, all units are in SI. However, to correspond with industry standards, flux is reported in litres per square metre per hour, pressure is reported in bar and permeability is reported in litres per square metre per hour per bar. All tests were operated with the stir bar rotating at 500 rpm, giving rise to an estimated mass transfer coefficient of $4 \times 10^{-5} \frac{m}{s}$ [12]. The effective area of the membrane was taken to be 14.38 cm^2 , determined via measurement with calipers.

For each test pressure, the experimental procedure consisted of three steps: a salt rejection test to insure minimal salt leakage around the membrane; a permeability test with DI water; and, a second salt rejection test to insure there is still minimal leakage around the membrane. In total, the three steps were designed to last 8 hours, which was estimated, from previous tests, to have been the representative time over which the most significant change in membrane permeability occurred. Salt rejection tests were run over a period of 45 minutes at the test pressure using 200 mL of 1 g/L sodium sulfate solution for the 34.5 bar (500 psi) test, and 300 mL of 1g/L sodium sulfate solution for the 103.4 bar (1500 psi) and 172.4 bar (2500 psi) test. During this 45 minutes, permeate was collected for 30 minutes and thrown away. Permeate was then collected for 15 more minutes and the conductivity of this permeate was measured using a Jenco 3250 conductivity meter and used to determine rejection. For permeability testing with DI water between the salt rejection tests, the cell was first rinsed with DI water and then filled with 300 mL of DI water. When 280 g of permeate had been gathered, the test would be stopped to refill the cell with DI water.

Modelling

The viscoelastic model proposed is similar in form to that employed in literature for NF membranes [5]. Essentially, the level of compaction (strain) of the active layer was modelled via a spring and a damper that are connected in parallel (Eq. 2).

$$\text{Eq. 2: } P = Kx + C\dot{x}$$

P is the applied pressure in Pa, K is a spring constant in Pa/m and C is a damper constant in Pa s/m. x is the active layer strain, defined as the change in thickness divided by its initial thickness. The solution to this equation takes the form:

$$\text{Eq. 3: } x = \left(x' - \frac{P}{K}\right) \exp\left(-\frac{Kt}{C}\right) + \frac{P}{K}$$

x' is the initial level of strain, which is zero at the very start of an experiment, and t is the time elapsed. Essentially, this model predicts that, when a constant pressure is applied, strain will rise to an asymptotic value, and, the higher the pressure, the higher the asymptotic strain. When no pressure is applied, the strain should return to zero, with the speed of return determined by the damper constant C .



To relate strain to flux, we assume a linear relationship between the change in permeability and the strain, as indicated in Eq. 4 [11]. In other words, if permeability drops by 10% relative to its initial value, we assume that strain has increased by 10%:

$$\text{Eq. 3: } 1 - \frac{A_m}{A_m^0} = x$$

where A_m^0 is the permeability measured after the initial application of pressure.

III. RESULTS AND DISCUSSION

Figure 1 illustrates the water flux of the RO membrane at three different pressures demonstrating that flux increases monotonously with the level of applied pressure. The first discontinuity in data for each pressure is as a result of stopping the test to switch out the sodium chloride solution for DI after the salt rejection test. Conversely, the last discontinuity in data for each pressure results from the DI water being swapped out for a sodium chloride solution after the DI water tests. Discontinuities in data during DI water tests result from the tests being stopped to refill the feed-water chamber with DI water. As was reported for NF membranes [4], it appears that there is a limiting flux, somewhere close to 172 bar, beyond which further increases in applied pressure yield no further increase in permeability. Interestingly, the value of applied pressure at which the limiting flux appears to be reached for the SWC RO membrane is much higher than was reported for the NF-90 membrane [4].

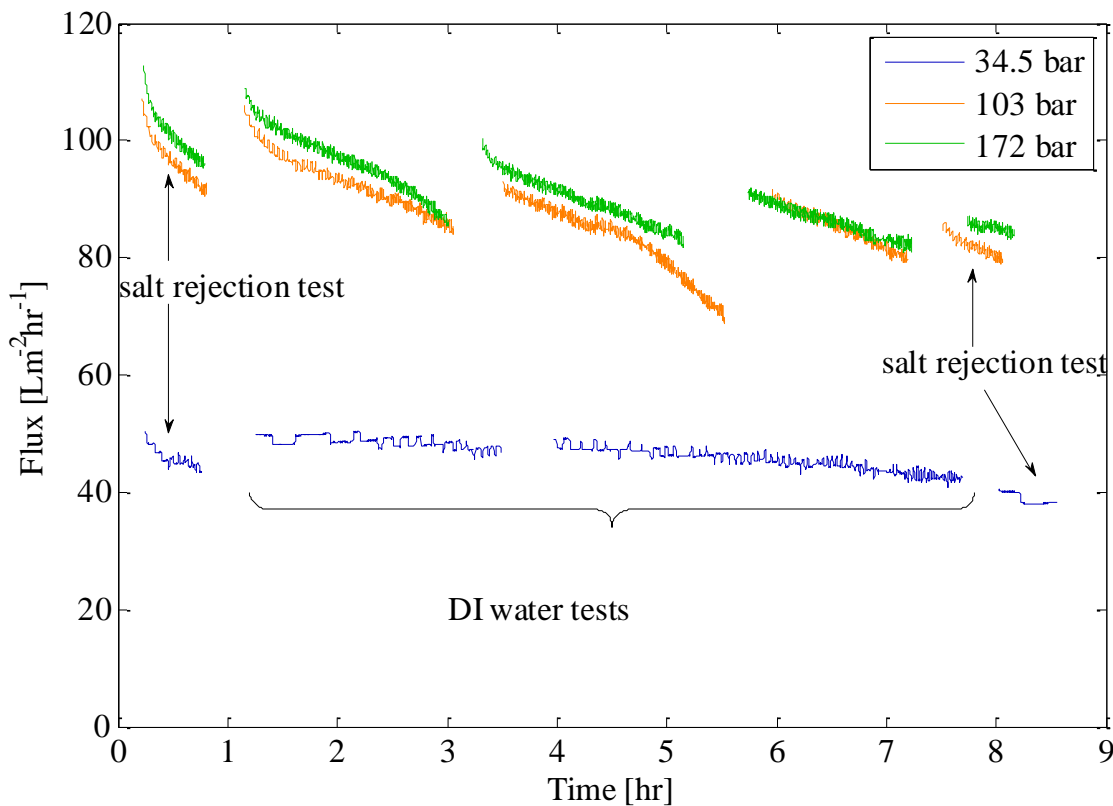


Fig. 1 Membrane flux versus time. Flux measurements during the processing of DI water are accurate to within 1.0% - calculated via the propagation of error from measuring the rejection rate of sodium sulfate. Flux measurements during salt rejection tests are accurate to within $\pm 5\%$, due to large error in estimating the mass transfer coefficient. Breaks in the data are due to the procedure needing us to change the water since the stirred cell we used does not have a large enough capacity to handle 7 hours of discharge. They are that large because we need 750 seconds of raw data to get our averaged data.

Figure 2 is derived from the combination of data in Figure 1 with data on the evolution of pressure with time. It illustrates the effect of applied pressure upon permeability – clearly illustrating how higher applied pressures lead to reduced membrane permeability. At a pressure of 172 bar, the permeability is less than half of the value at 34.5 bar. This no doubt implies that reverse osmosis systems operating at higher pressures can be expected to require greater membrane area, a greater number of pressure vessels and a larger footprint than conventional seawater desalination systems.

Of particular note, both in Figs. 1 and 2, is the recovery of flux and permeability when pressure is released – even for a brief period – and then reapplied. Although pressure is removed for only a matter of minutes when the DI water in the cell is refilled, there is a very notable increase in flux and permeability when the pressure is reapplied; it is clear that some form of viscoelastic behavior is at play in the membrane. To better understand this behavior, the spring-damper model described in the methods was fitted to the data for DI water processing in Fig. 2. Although the model fits the data reasonably well over the full eight hours it does not accurately predict the rapid recovery of permeability when pressure is removed. It seems that either the spring-damper model chosen, or the assumptions relating permeability to strain are not fully satisfactory.

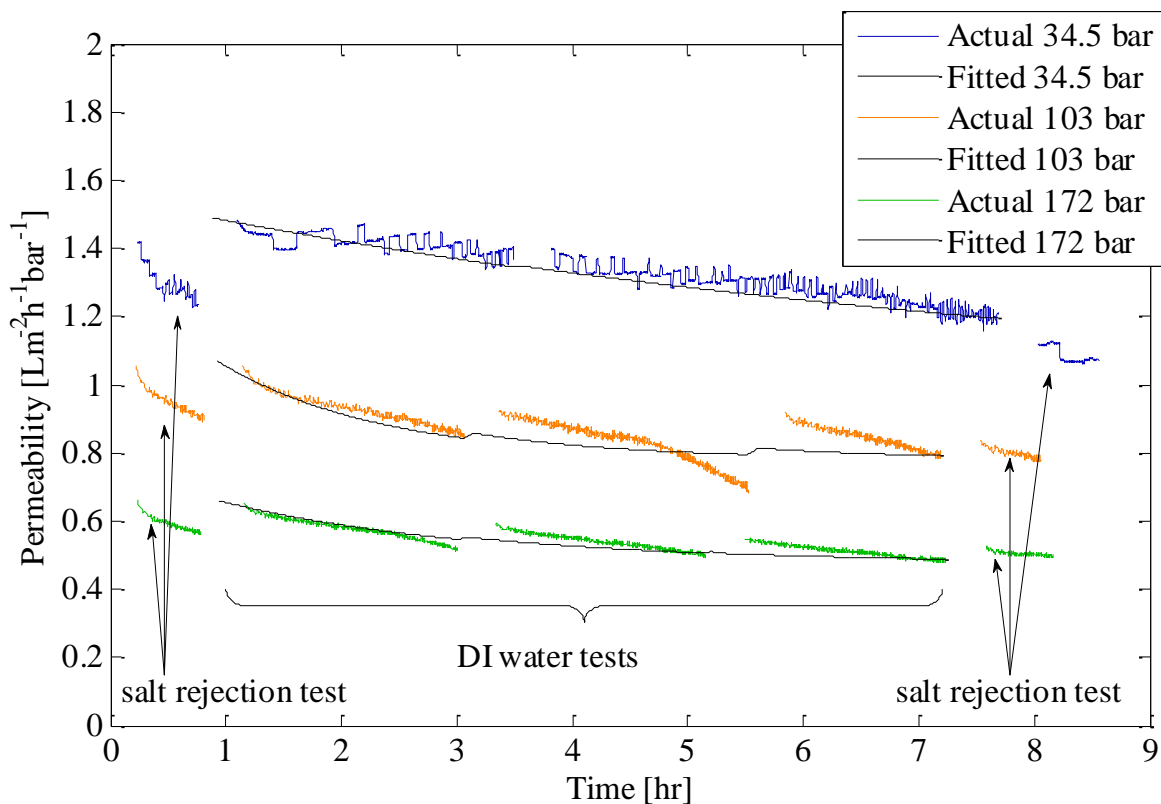


Fig. 2 Membrane permeability versus time. The error on permeability measurements, propagated from error on measuring flux and pressure, is $\pm 1.0\%$. Breaks in the data are due to the procedure needing us to change the water since the stirred cell we used does not have a large enough capacity to handle 7 hours of discharge. They are that large because we need 750 seconds of raw data to get our averaged data.

Finally, the salt rejection rates corresponding to Figs. 1 and 2 are shown in Table 1. The level of leakage around the O-ring is difficult to quantify and, therefore, these values of rejection serve only as a lower bound upon the true rejection of the membrane. Furthermore, these values of rejection are specific only to a single run at each pressure, i.e. if the test at 34.5 bar were to be repeated, we would expect variance in the rejection at the start and end due to stochastic differences in the seal between the membrane and the O-ring as well as possible differences in the membrane sample itself because of the non-uniformity of membrane sheets [4]. For this reason, while we can legitimately compare rejections at the start and end of the same test, it is more difficult to compare the rejections obtained at different pressures. Notwithstanding these limitations, there is nonetheless an important increase in membrane rejection with time in the tests conducted at each of the three pressures, as was previously reported for NF membranes [5], indicating that membrane compaction tends to boost rejection.

Table 1, Salt rejection at the start and end of three runs at different pressures. In each case, the error on conductivity measurements results in an uncertainty of 0.01% on rejection.

Pressure [bar]	Start	End
34.5	98.74%	99.13%
103	98.96%	99.76%
172	98.10%	99.62%

V. CONCLUSIONS

We have demonstrated, experimentally, that a seawater reverse osmosis membrane (SWC, Hydranautics) can maintain excellent salt rejection when operating at pressures of up to 172 bar. While we have shown that RO is technically feasible up to at least 172 bar, we have also shown that the permeability at such pressure falls by more than 50% relative to its value at 34.5 bar. If this membrane were to be used, the RO system would therefore be at least twice as large, in terms of membrane area and footprint, as a seawater RO system that produced permeate at the same rate. Furthermore, given the apparent viscoelastic nature of the reverse osmosis membrane, operators of high pressure RO systems should expect high variability in permeate flow rates with time, even if the applied pressure is held fixed in time. Still, the potential benefits, especially in terms of reduced energy consumption, of replacing technologies such as mechanical vapor compression with high pressure reverse osmosis are very significant. We therefore believe that high pressure reverse osmosis holds great promise for the near future.

VI. REFERENCES

1. Shaffer, Devin L., Laura H. Arias Chavez, Moshe Ben-Sasson, Santiago Romero-Vargas Castrillón, Ngai Yin Yip, and Menachem Elimelech. "Desalination and reuse of high-salinity shale gas produced water: drivers, technologies, and future directions." *Environmental science & technology* 47, no. 17 (2013): 9569-9583.
2. Mistry, Karan H., Ronan K. McGovern, Gregory P. Thiel, Edward K. Summers, Syed M. Zubair, and John H. Lienhard. "Entropy generation analysis of desalination technologies." *Entropy* 13, no. 10 (2011): 1829-1864.



3. Thiel, Gregory P., Emily W. Tow, Leonardo D. Banchik, Hyung Won Chung, and John H. Lienhard. "Energy consumption in desalinating produced water from shale oil and gas extraction." *Desalination* (2015).
4. Hussain, Yazan A., Mohammed H. Al-Saleh, and Suekainah S. Ar-Ratrout. "The effect of active layer non-uniformity on the flux and compaction of TFC membranes." *Desalination* 328 (2013): 17-23.
5. Hussain, Yazan A., and Mohammed H. Al-Saleh. "A viscoelastic-based model for TFC membranes flux reduction during compaction." *Desalination* 344 (2014): 362-370.
6. Luk-Cyr, Jacques. "Experiments and modeling of multilayered coatings and membranes: application to thermal barrier coatings and reverse osmosis membranes." PhD diss., Massachusetts Institute of Technology, 2014.
7. Roh, Il Juhn, Jae-Jin Kim, and Soo Young Park. "Mechanical properties and reverse osmosis performance of interfacially polymerized polyamide thin films." *Journal of membrane science* 197, no. 1 (2002): 199-210.
8. Tang, Chuyang Y., Young-Nam Kwon, and James O. Leckie. "Effect of membrane chemistry and coating layer on physiochemical properties of thin film composite polyamide RO and NF membranes: I. FTIR and XPS characterization of polyamide and coating layer chemistry." *Desalination* 242, no. 1 (2009): 149-167.
9. Tang, Chuyang Y., Young-Nam Kwon, and James O. Leckie. "Effect of membrane chemistry and coating layer on physiochemical properties of thin film composite polyamide RO and NF membranes: II. Membrane physiochemical properties and their dependence on polyamide and coating layers." *Desalination* 242, no. 1 (2009): 168-182.
10. Coronell, Orlando, Benito J. Marinas, and David G. Cahill. "Depth heterogeneity of fully aromatic polyamide active layers in reverse osmosis and nanofiltration membranes." *Environmental science & technology* 45, no. 10 (2011): 4513-4520.
11. Van Der Velden, P. M., and C. A. Smolders. "Initial flux decline and initial rejection increase for swollen ionic membranes." *Journal of Applied Polymer Science* 20, no. 5 (1976): 1153-1164.
12. Becht, Nils O., Danish J. Malik, and E. S. Tarleton. "Evaluation and comparison of protein ultrafiltration test results: dead-end stirred cell compared with a cross-flow system." *Separation and purification technology* 62, no. 1 (2008): 228-239.

